The Armed Forces Institute of Pathology
Department of Veterinary Pathology

Conference Coordinator:
Shannon Lacy, DVM, MPH

WEDNESDAY SLIDE CONFERENCE 2009-2010

Conference 7

28 October 2009

Conference Moderator:

Mark A. Bryant, DVM, Diplomate ACVP

CASE I: RAT (AFIP 3139909).

Signalment: Young, adult, female Sprague-Dawley rats (*Rattus norvegicus*).

History: At necropsy, multiple asymmetrical nodules were present in the uterine body of young adult female control rats.

Gross Pathology: Multiple asymmetrical nodules were present in the uterine body of several control rats. Nodules were submitted for microscopic examination as incidental lesions.

Histopathologic Description: In the mesometrial side of the uterus, there is an expansile, partially encapsulated nodular mass composed of three poorly defined zones or layers of pleomorphic cells asymmetrically centered on a dilated endometrial gland lumen (not visible in all sections). From the periphery of the nodule, just deep to capsule, the mesometrial zone is composed of an irregular, thin, poorly demarcated band of small spindle-shaped cells with poorly defined cell borders, finely vacuolated basophilic to amphophilic cytoplasm and small oval nuclei ("spiny" cells). Deep to the mesometrial zone, also on the mesometrial aspect of the uterine horn, there are clusters and nests of variably sized (approximately 30 to 50 um diameter) cells composing the transition zone characterized by more abundant coarse clear cytoplasmic vacuoles, round, finely vesicular nuclei and abundant basophilic to amphophilic cytoplasm ("glycogenic" area). Intermixed with the cells in this mesometrial zone, there are numerous larger cells containing coarse, deeply eosinophilic cytoplasmic granules (PAS not available). Deep to this zone, approaching the uterine lumen and partially surrounding the endometrial gland lumen, there are clusters of large (approximately 120 to 150 um), pleomorphic, coarsely vacuolated epithelioid giant cells containing coarsely vesicular chromatin in large oval nuclei with one to four variably shaped nucleoli and abundant coarsely granular amphophilic to basophilic cytoplasm (decidual cells). Deep to and partially surrounding these cells, there is an irregular layer of nests and clusters of small, occasionally multinucleate or binucleate cells with small, central, oval nuclei containing finely vesicular chromatin and a single small eccentric nucleolus (antimesometrial basal zone). The cells of the nodule are supported on a fine fibrovascular stroma (compressed endometrial stroma) with numerous small congested blood vessel profiles. There is erosion

*Sponsored by the American Veterinary Medical Association, the American College of Veterinary Pathologists, and the C. L. Davis Foundation.

of the overlying endometrial surface, focally, with small numbers of degenerate neutrophils perivascularly and at the endometrial surface (not present in all sections).

Contributor's Morphologic Diagnosis: Uterus: Decidual alteration (deciduoma).

Contributor's Comment: Decidual alteration or reaction, also referred to as a deciduoma, is an infrequent, self-limiting, proliferative but not neoplastic entity in young adult female rats. Decidual alteration has been observed in the guinea pig, rabbit, mouse, dog, hamster and monkey.[4] The incidence of decidual alteration in this control group was unusual in our experience. Although slides and sections varied in submitted material, decidual alteration comprises a fairly structured architecture/organization, as described above. Elcock and co-authors, in *Monographs on Pathology of Laboratory Animals: Genital System* provide detailed histologic and ultrastructural descriptions of deciduoma/decidual alteration.[4]

Decidual alteration was referred to as deciduoma in earlier lab exploratory pathology literature because the lesion was originally regarded as neoplastic.[5] Instead, this is a proliferative, well organized structure that generally follows a predictable time-course. The alteration can be induced between days 3 and 4 of pseudopregnancy, and requires priming or sensitization of the uterus by progesterone for at least 48 hours, followed by minute amounts of estrogen.[4] Most often, this sequence of events is linked to the late luteal phase of the estrus cycle.[5,6] Decidual alteration in the rat has also been reported following various forms of mechanical irritation or trauma, electrical stimulation, intrauterine instillation of agents such as sesame oil, Hank's balanced salt solution, histamine, air, or prostaglandins, as well as administration of progestin, such as 19-norpregnane.[4,5] The alteration will generally undergo regression between days 12-16 (nodular form) and 21 (diffuse form) of pseudopregnancy, with necrosis and cleavage of the capsule from the underlying uterine wall.[4]

Decidual alteration occurs spontaneously in rats, usually at a low incidence (<1% over a 10 year period in one study).[4] The incidence in this group of young adult control rats was unusual in our experience. According to Elcock et al., vitamin E deficiency may be a contributing factor to increased spontaneous incidence of deciduoma, with 60% of rats fed vitamin E deficient diets developing spontaneous deciduoma compared with 4% on natural food.[4]

AFIP Diagnosis: Uterus: Exuberant myometrial and stromal decidualization with maternal and embryofetal placental structures.

Conference Comment: This edifying case elicited a vivacious discussion during the conference, and was therefore subsequently reviewed in consultation with several veterinary pathologists with special expertise in laboratory animal and/or reproductive pathology. While a unified consensus on the histogenesis of this incidental finding was not achieved, several possibilities were raised, with many suspecting a placental disk consistent with normal pregnancy. Deciduoma and pregnancy are mutually exclusive diagnoses; deciduoma accompanies pseudopregnancy as noted by the contributor, while myometrial and stromal decidualization is an expected physiologic response to normal pregnancy, and is accompanied by placental tissues of embryofetal origin. In many slides, a large proportion of the nodule consists of placental tissues not of maternal origin.

Although participants recognized exuberant decidualization in the mesometrial aspect of the uterus, characterized by the ubiquitous presence of large, pale, glycogen-rich decidual cells in the myometrium and stroma, many could not discern the six components of a classic deciduoma, i.e. metrial gland in the myometrium on the mesometrial side of the uterus, basal zone separating the deciduoma from the myometrium, a capsule just luminal to the basal zone, mesometrial and antimesometrial regions, and a "glycogenic" transitional area.[6] Rather, participants noted five distinct layers in the mesometrial aspect of the uterus that, collectively, are interpreted as structures of a placental disk (**fig. 1-1**). Notably, the characteristic layers are not described as part of a deciduoma. From adluminal to luminal, they are:

1. Decidualized myometrium: The mesometrial myometrium is composed of large decidual cells with abundant, slightly basophilic, vacuolated cytoplasm that often contains PAS-positive granules, round nuclei and one or two distinct nucleoli. Larger vessels within the decidualized myometrium are surrounded by numerous metrial cells, and the endothelium is often covered by large cytotrophoblasts (**fig. 1-2**).
2. Decidualized stromal layer: Separated from the decidualized myometrium by a discontinuous, indistinct, thin band of myometrial smooth muscle cells is a completely decidualized stromal layer; this layer is composed of decidual cells as described in the myometrium, with clear cytoplasmic vacuoles that become progressively prominent toward the luminal surface.
3. Giant cell layer: A layer of giant trophoblasts separates maternal-origin tissue (decidua) from embryofetal-origin tissue. Giant trophoblasts are

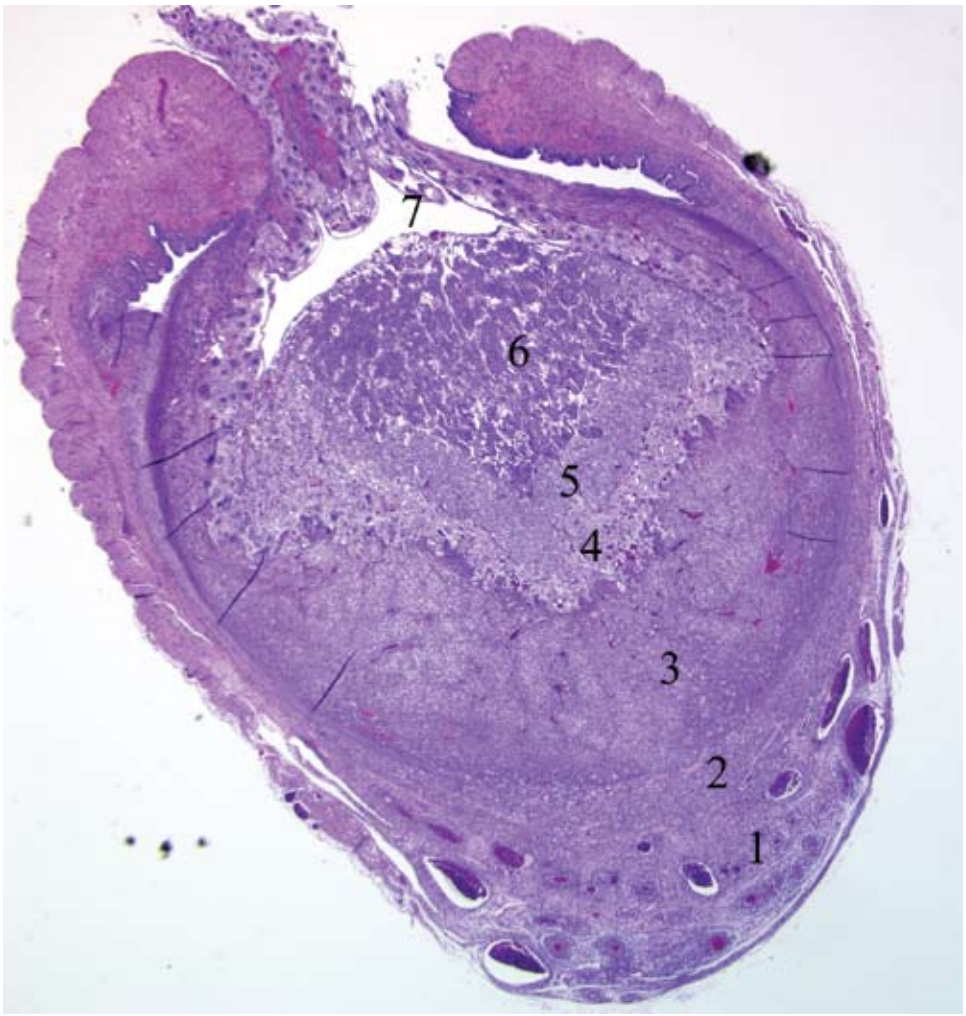

1-1. Uterus, rat. Distinct areas within the affected segment of uterus are evident. From anti-mesometrial to mesometrial, these are: Metrial gland (1), decidualized myometrium (2), stromal layer (3), layer of giant trophoblasts (4), trophospongium (5), labyrinth (6), and yolk sac (7). (HE 12.5X)

up to 150 um in diameter and have abundant, finely-granular, microvacuolated, pale basophilic cytoplasm that often contains distinct PAS-positive droplets. Nuclei are large and round to oval with finely-stippled or coarsely-clumped chromatin and contain one to ten distinct, variably-sized, irregularly-shaped nucleoli (**fig. 1-3**).

4. Trophospongium: Interposed between the giant cell layer and the labyrinth is a band of 20-40 um diameter polygonal cells with moderate amounts of basophilic, vacuolated cytoplasm containing numerous small, PAS-positive granules; these cells are often bi-nucleate with frequent mitoses. Groups of cells comprising this population are separated by fewer large (60-80 um diameter) syncytiotrophoblasts and small vascular lacunae containing mature erythrocytes.
5. Labyrinth: The luminal-most layer of the mesometrial side of the uterus is composed of trophoblasts arranged in trabeculae that separate large and small blood-filled lacunae. Trophoblasts contain moderate amounts of basophilic, microvacuolated cytoplasm, and are mitotically active. Larger lacunae contain mature erythrocytes (maternal circulation), while smaller lacunae contain only large, immature, nucleated erythrocytes with pale eosinophilic to basophilic cytoplasm (fetal circulation). Generally, maternal and fetal lacunae are separated by three layers of trophoblasts (hemotrichorial placentation) (**fig. 1-4**).

In the affected rats of this case the yolk sac placenta is present in the uterine lumen in most histologic sections, which consists of a single layer of plump, cuboidal, luminally-oriented cells resting on a 2-5 um thick, glassy, hyaline basement membrane (Reichert's membrane) (**fig. 1-5**). Employing the morphologic reference data set provided by de Rijk and colleagues [2] as a guide, the placental features described above are interpreted as consistent with a placenta at approximately day 12-14 of pregnancy. However, not all of these features are present on every section, and most slides have two sections,

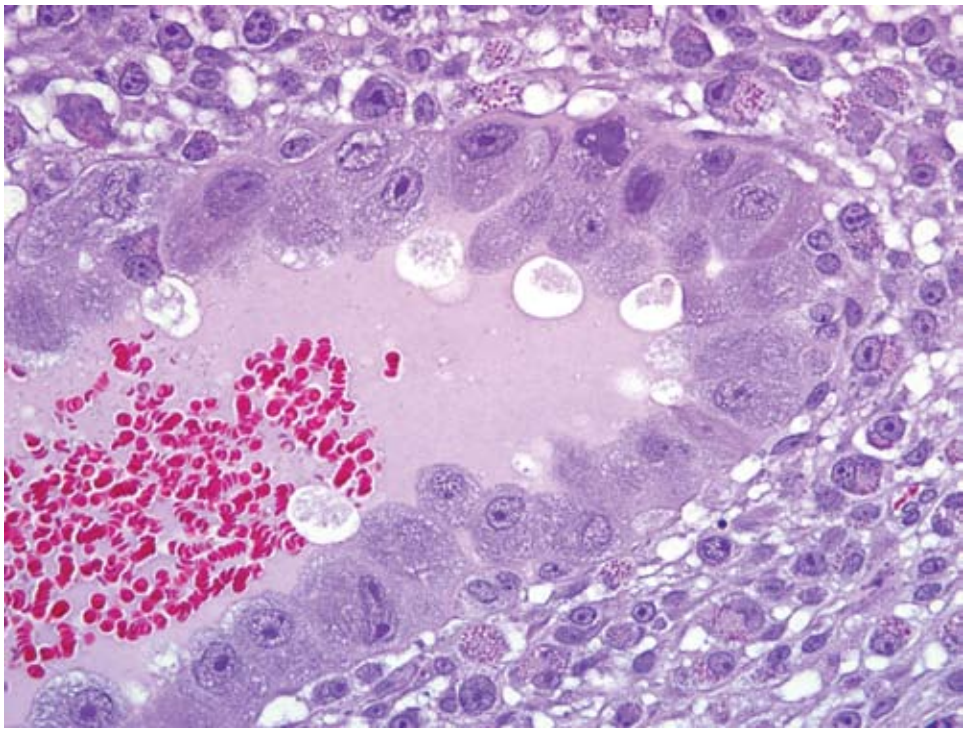

1-2. Uterus, rat. The endothelial cells of vessels within the myometrium are invested by trophoblasts. (HE 400X)

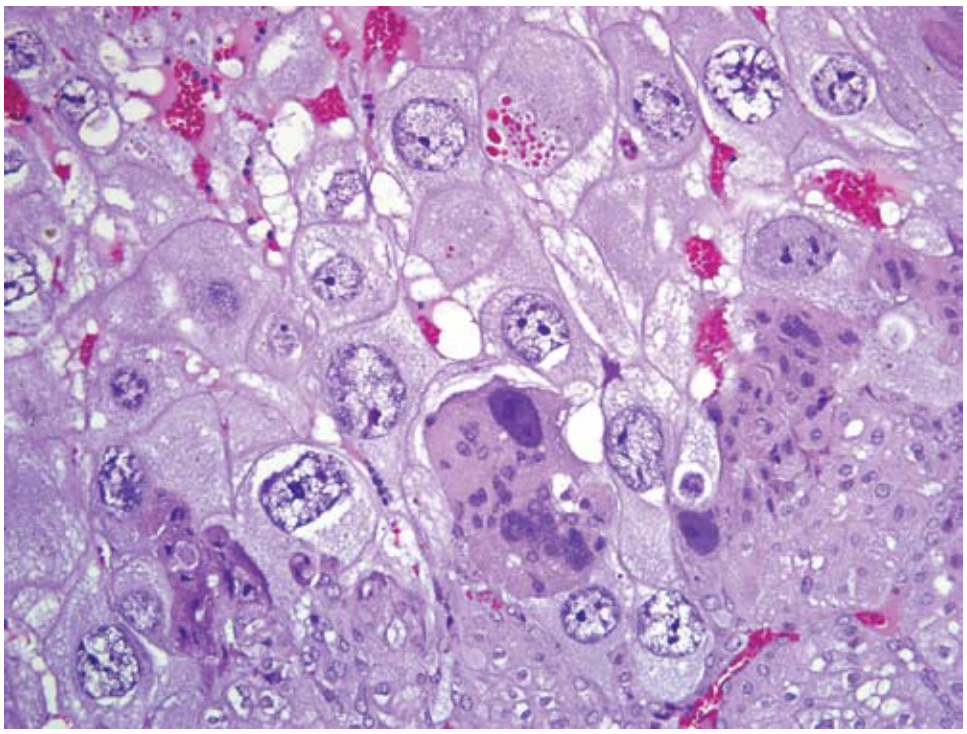

1-3. Uterus, rat. The layer of giant trophoblasts invades the decidualized stroma. (HE 400X)

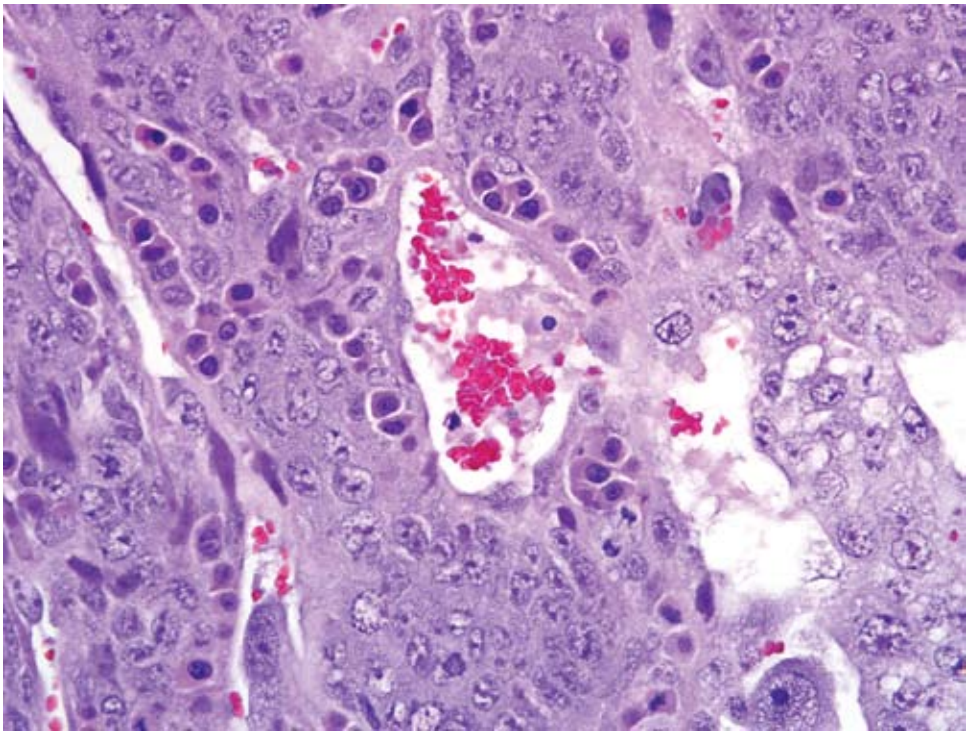

1-4. Uterus, rat. Within the labyrinth, there are large lacunae containing mature anucleate maternal erythrocytes that are separated from smaller lacunae by up to three layers of syncytiotrophoblasts; smaller lacunae contain more basophilic nucleated fetal erythrocytes. (HE 400X)

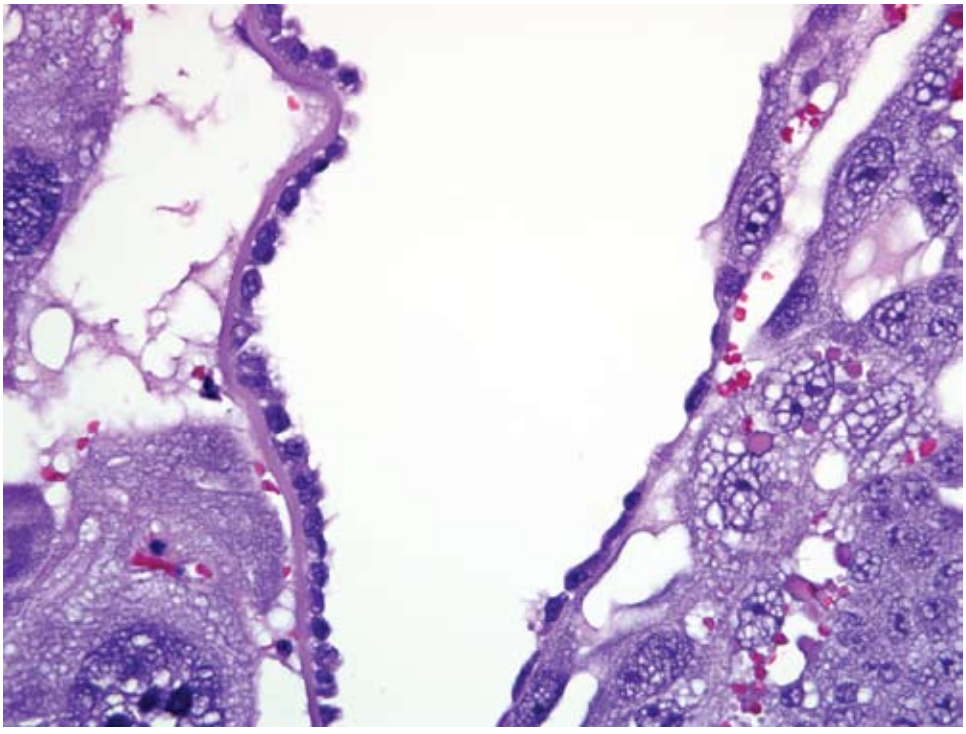

1-5. Uterus, rat. The yolk sac is lined by plump yolk sac epithelium which rests on a glassy, hyalinized membrane (Reichert's membrane). (HE 400X)

one of which lacks the giant cell layer, trophospongium, labyrinth, and yolk sac altogether. Additionally, other features of a normal rat pregnancy, i.e. a conceptus and fetal umbilical vessels, are conspicuously absent. One possible explanation for the presence of both maternal and embryofetal placental structures in the absence of a conceptus is embryonic death. For example, embryonic death attributed to an intercurrent infection with Sendai virus and *Pasteurella pneumotropica* resulted in the formation of deciduomas with trophoblastic giant cells in rats (1); admittedly, this unlikely scenario does little to account for the clinical history in this case, and would likely result in significantly more placental pathology than is present in the examined sections.

In light of the lively discussions elicited by this case, the contributor was contacted to confirm the case history and ensure the possibility of pregnancy was excluded. Indeed, the submitted specimens were sampled from several female control rats that were pair-housed in a long-term study, and pregnancy would have been self-evident given the length of the study. Anecdotally, some experienced pathologists have noted extremely well-organized decidual reactions like this in rats that were certainly not pregnant; unfortunately, such examples are not reported in the literature, and we are unable to explain the presence of placental components of apparent fetal origin. A parthenogenetic process was also considered as a possible cause, but deemed exceedingly unlikely in this case given the signalment and clinical history provided by the contributor. Thus, we conclude that the histologic findings are most compatible with pregnancy and very recent embryonic loss. However, these histologic features in a known unmated animal are unique in our experience, and the pathogenesis remains unclear. We extend our sincere thanks to the contributor for submitting this very interesting case, and to the veterinary pathologists who graciously shared their opinions and expertise.

Contributor: Wyeth Research, Department of Pathology, 641 Ridge Road, Chazy, New York 12921
http://www.wyeth.com

References:

1. Carthew P, Aldred P: Embryonic death in pregnant rats owing to intercurrent infection with Sendai virus and *Pasteurella pneumotropica*. Lab Anim **22**:92-97, 1988
2. de Rijk EPCT, van Esch E, Flik G: Pregnancy dating in the rat: placental morphology and maternal blood parameters. Toxicol Pathol **30**:271-282, 2002
3. Elcock LH, Stuart BP, Mueller RE, Hoss HE: Deciduoma, uterus, rat. *In:* Monographs on Pathology of Laboratory Animals: Genital System, eds. Jones TC, Mohr U, Hunt RD, pp. 140-145. Springer-Verlag, Berlin Heidelberg, 1987
4. Greaves P: Female genital tract. *In:* Histopathology of Preclinical Toxicity Studies: Interpretation and Relevance in Drug Safety Evaluation, 3rd ed., pp 728-29. Elsevier, London, UK, 2007
5. Leininger JR and Jokinen MP: Oviduct, uterus and vagina. *In:* Pathology of the Fischer Rat: Reference and Atlas, eds. Boorman GA, Eustis SL, Elwell MR, Montgomery Jr. CA, MacKenzie WF, pp. 450-52. Academic Press, Inc., London, UK, 1990

CASE II: 34 (AFIP 2936324).

Signalment: 1.5-year-old, male knockout mouse (specific mutation not provided) (*Mus musculus*).

Gross Pathology: In mice older than 8 months, the stomach was contracted and contained scant ingesta. The wall of the glandular stomach was pale, markedly thickened, and formed prominent folds apparent from the serosal and mucosal aspects (**fig. 2-1**).

Histopathologic Description: Stomach: The normal glandular mucosa is completely replaced by hyperplastic mucosa. Chief cells and parietal cells are virtually absent and the distinction between the cardiac, fundic, and pyloric regions is lost. The abnormal mucosa is very tall and measures approximately 900-1800 um in thickness. By comparison, in wild-type (WT) controls, the fundic mucosa is approximately 450 um (300-700 um) thick and the pyloric mucosa is 250 um (200-350 um) thick. There is pronounced elongation of the gastric pits and glands, which are lined by two (or three, see below) epithelial cellular types (**fig. 2-2**). In the basal mucosa, the lining cells are cuboidal to columnar with pale, wispy cytoplasm and resemble lining cells of the normal mucous glands in the antral/pyloric mucosa. In the adlumenal region, two intimately admixed cell types are seen: one population is cuboidal to columnar with amphophilic to eosinophilic cytoplasm and is similar to normal surface epithelial cells/pit cells. The second population, which apparently arises from the latter and is very common in this specimen, is tall columnar with homogenous brightly eosinophilic cytoplasm, so-called hyaline change,[1] hyalinosis, or eosinophilic cytoplasmic change.[2] The hypereosinophilic

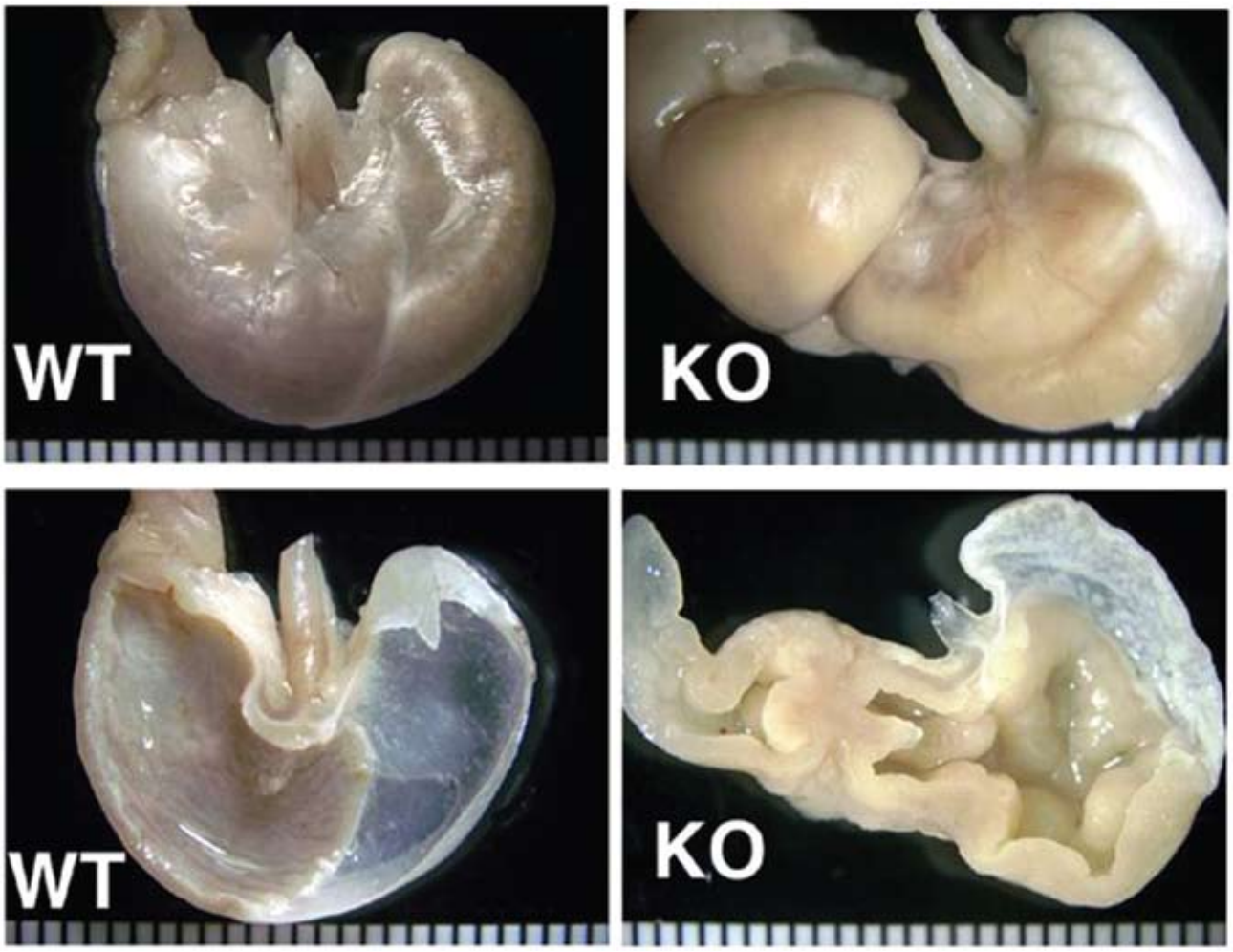

2-1. Stomach, mouse. The wall of the glandular stomach was pale, markedly thickened, and formed prominent folds apparent from the serosal and mucosal aspect (affected mouse on right, normal on left). Photograph courtesy of Weizmann Institute of Science, Department of Veterinary Resources, Rehovot 76100, Israel, www.weizmann.ac.il

material either forms a discrete globular accumulation within the cytoplasm or fills it entirely. There is scattered cytoplasmic vacuolation in the hyperplastic and often hypertrophic pit cells. Large aggregates of rectangular acicular and globular hypereosinophilic crystalline material are commonly seen within distended lumena of hyperplastic pits, at times with a small amount of cellular debris (**fig. 2-3**). There is multifocal cystic dilation predominantly of the glands, with multifocal 'herniation' into subjacent layers up to, but not through, the serosa. There is mild multifocal lymphoplasmacytic and eosinophilic lamina proprial and submucosal infiltration with occasional accumulation of granular yellow-brown pigment-laden macrophages. In some areas there is epithelial erosion with neutrophilic infiltration and bacterial colonies. There is mild to moderate multifocal fibrosis of the lamina propria. Mitotic figures are commonly seen. Dysplastic foci are occasionally recognized and exhibit atypia in the form of nuclear pleomorphism, nuclear stratification, loss of nuclear polarity, increased nuclear to cytoplasmic ratio and hyperchromasia. In some sections, polypoid mucosal masses are present and exhibit pronounced dysplasia, marked mixed inflammatory infiltration and advanced fibrosis. The pylorus (not present on all slides) is dilated and hyperplastic mucosa bulges into and distends the duodenal lumen. The villi in this region are nearly completely effaced. The mucosa overlying Brunner's gland is abnormal and similar to the hyperplastic gastric mucosa (metaplasia). More distally, there is marked infiltration of the lamina propria by lymphocytes, plasma cells, eosinophils and granular yellow-brown pigment-laden macrophages. Mucosal architecture is distorted with

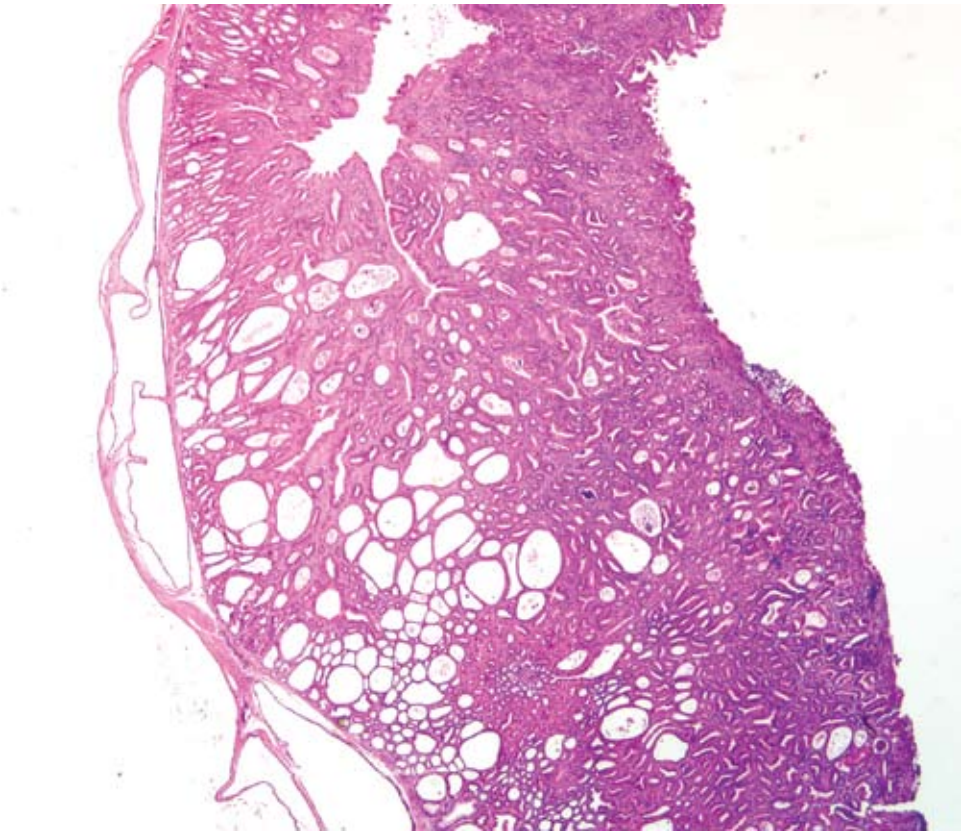

2-2. Stomach, mouse. Diffusely, the mucosa is markedly hyperplastic, forming tubular and cystic spaces which often extend through the muscularis mucosa and occasionally through the tunica muscularis. (HE 20X)

prominent villous blunting and fusion, crypt elongation and goblet cell hyperplasia. There are scattered crypt abscesses. In the forestomach, there is diffuse moderate thickening of the keratin layer and minimal multifocal mononuclear and eosinophilic infiltration.

Contributor's Morphologic Diagnosis:

1. Stomach (glandular portion): Severe diffuse adenomatous hyper–plasia with hyalinosis, mild to moderate multifocal mononuclear, eosinophilic and erosive gastritis.
2. Stomach (squamous portion): Moderate diffuse orthokeratotic hyperkeratosis.
3. Proximal duodenum: Mucosal metaplasia with hyalinosis, moderate to marked diffuse chronic-active lymphoplasmacytic and eosinophilic enteritis.

Contributor's Comment: In mice, hyperplasia of the glandular mucosa with variable degrees of inflammatory infiltration is a heterogeneous condition known by several alternative designations: adenomatous hyperplasia, gastric hyperplasia, fundic mucosal hyperplasia, giant hypertrophic gastritis, hypertrophic gastropathy, chronic gastritis and proliferative gastritis.[1,4,7] Conditions in which this lesion is encountered include the following:

i. As a spontaneous lesion in several mouse strains including Han:NMRI,[14] strain I,[1] aging C57BL/6x129 and 129/Sv mice[2] and CD-1 mice.[3]
ii. In experimental infection with *Helicobacter felis* of WT C57BL/6 mice[5] and several mutant strains (e.g. IL-10-/-).
iii. With long-term treatment of mice with H_2 blocking drugs [13] and other antisecretory compounds.[1]
iv. In experimental infection of immunodeficient mice with *Taenia taeniaformis*.[8]
v. In several knockout and transgenic mice.[10]
vi. In densely housed mice.[7]
vii. In association with colitis in mutant mice.[4,5]

The gastric hyperplasia observed in the above conditions may have distinguishing gross and/or histologic features depending on the specific etiology. Common to these is mucosal hyperplasia with loss of specialized cells, also referred to as mucous metaplasia. The degree of

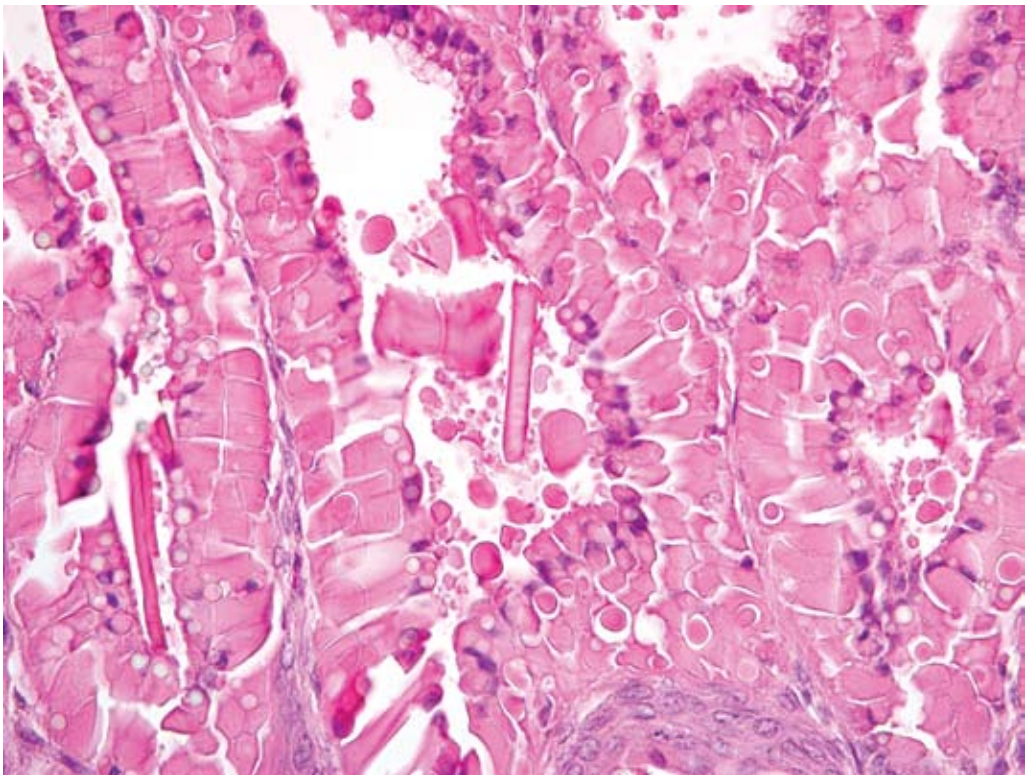

2-3. Stomach, mouse. Multifocally, dilated crypts in the hyperplastic mucosa contain brightly eosinophilic crystalline material. Epithelial cells often contain intracytoplasmic, 10-15 um spherical globules of pale to brightly eosinophilic material. (HE 400X)

inflammatory infiltration is variable. In the gastric lesion from this knockout, the degree of hyperplasia clearly outstrips inflammation. Alcian blue and periodic acid Schiff stains demonstrate altered mucin production, as expected.[7] The extent of hyalinosis in this case is striking. The globular hypereosinophilic material was strongly immunoreactive with a polyclonal antibody raised against Ym1/T-lymphocyte-derived eosinophil chemotactic factor (immunohistochemical staining kindly provided by JM Ward, NCI). Proteins in this family are believed to play a role in mucosal defense against parasites.[15]

The cause of the lesion in this knockout, as in many of the above, remains undetermined. In some cases it may be due to hormonal imbalance, e.g. hypergastrinemia. The hyperkeratosis in the forestomach is consistent with insufficient mechanical abrasion of keratin due to reduced food intake.[3] The proliferative enteritis in the proximal duodenum is always encountered in conjunction with the gastric lesion, to which it is assumed to be secondary. While in man metaplasia of the gastric mucosa is associated with an increased risk of carcinoma, the murine condition is often not associated with increased incidence of gastric malignancy.[3,14]

In domestic animals, conditions which bear some resemblance to this lesion include giant hypertrophic gastritis (Menetrier's disease) in dogs and chronic abomasitis with mucous metaplasia in ruminants caused by infestation with *Ostertagia* sp. ("Morocco leather").

AFIP Diagnosis: 1. Stomach, glandular: Hyperplasia, adenomatous, diffuse, marked, with cystic mural herniation, chief and parietal cell loss, epithelial hyalinosis, mucous metaplasia acicular eosinophilic crystalline material, and mild multifocal eosinophilic and neutrophilic gastritis.
2. Stomach, squamous: Hyperkeratosis, orthokeratotic, diffuse, moderate.

Conference Comment: In addition to the gastric lesions described above, participants' slides contained an array of duodenal changes, ranging from proliferative lesions to diffuse blunting and fusion of villi with chronic-active and eosinophilic inflammation. The contributor provides a concise summary of potential causes for gastric hyperplasia in mice. This case was submitted in 2004; more recently, long-term infection with *Helicobacter heilmannii* has been reported to cause mucosal nodular hyperplasia due to gastric epithelial proliferation in C57BL/6 mice. In contrast to the present case, affected mice developed mucosal and submucosal lymphoid follicles composed predominantly of CD45R+ cells.[12] Silver stains using the Warthin-Starry and Steiner's methods did not reveal an etiologic agent in this case.

During the conference, participants compared the slide for this case with a section of normal mouse stomach to emphasize the striking mucous metaplasia and hyalinosis present herein. Hyalinosis has been described in a variety of tissues and a variety of mouse strains. In the glandular stomach of affected 129S4/SvJae and B6;129 mice, the extracellular and eosinophilic crystals were determined to be composed of Ym2 protein, a chitinase-related protein. Other sites reportedly affected by hyalinosis in mice include biliary and pancreatic duct epithelium, and the respiratory epithelium lining the nasal cavity and respiratory tract.[15]

In addition to the examples cited by the contributor, conference participants discussed other instances of proliferative gastric lesions in domestic animals, including equine hypertrophic gastritis associated with *Habronema* spp. and *Trichostrongylus axei*, hypertrophic gastritis in nonhuman primates caused by *Nochtia nocti*, gastritis in pigs caused by *Hyostrongylus rubidus*, and gastritis in cats caused by *Ollulanus tricuspis*.[6] In addition to ostertagiosis, *Cryptosporidium andersoni* has been recognized as a cause of proliferative abomasitis in cattle.[11]

Contributor: Weizmann Institute of Science, Department of Veterinary Resources, Rehovot 76100, Israel
http://www.weizmann.ac.il/

References:

1. Betton GR, Whiteley LO, Anver MR, Brown R, Deschl U, Elwell M, Germann PG, Hartig F, Kuttler K, Mori H, Nolte T, Puscher H, Tuch K: Gastrointestinal tract. *In:* International Classification of Rodent Tumors, the Mouse, ed. Mohr U, p. 38. Springer-Verlag, Berlin, 2001
2. Ennulat D, Kawabe M, Kudo G, Peters JM, Kimura S, Morishima H, Gonzalez FJ, Ward JM: Hyperplastic gastric mucosal lesions with eosinophilic cytoplasmic inclusions in aging C57BL/6N x 129 and Sv/129 mice. Abstract Vet Path **35:**456, 1998
3. Faccini JM, Abbott DP, Paulus GJJ: Mouse Histopathology: a Glossary for Use in Toxicity and Carcinogenicity Studies, pp. 98-102. Elsevier, New York, NY, 1990
4. Fernandez-Salgureo PM, Ward JM, Sundberg JP, Gonzalez FJ: Lesions of aryl-hydrocarbon receptor-deficient mice. Vet Pathol **34:**605-614, 1997
5. Fox JG, Dangler CA, Schauer DB: Inflammatory bowel disease in mouse models: role of microintestinal microbiota as proinflammatory modulators. *In:* Pathology of Genetically Engineered Mice, eds. Ward JM, Mahler JF, Maronpot RR, Sundberg JP, pp. 302-303. Iowa State University Press, Ames, IA, 2000
6. Gelberg HB: Alimentary system. *In:* Pathologic Basis of Veterinary Disease, eds. McGavin MD, Zachary JF, 4th ed., pp. 339-341. Mosby Elsevier, St. Louis, MO, 2007
7. Greaves P, Boiziau JL: Altered patterns of mucin secretion in gastric hyperplasia in mice. Vet Pathol **21:**224-228, 1984
8. Lagapa JT, Konno K, Oku Y, Nonka N, Ito M, Kamiya M: Gastric hyperplasia and parietal cell loss in *Taenia taeniaformis* inoculated immunodeficient mice. Parasito Int **51:**81-89, 2002
9. Leininger JR, Jokinen MP, Dangler CA, Whiteley LO: Oral cavity, esophagus and stomach. *In:* Pathology of the mouse, eds. Maronpot RR, Boorman GA, Gaul BW, 1st ed., pp. 36-37. Cache River Press, Vienna, IL, 1999
10. Maehler M, Rozell B, Mahler JF, Merlino G, Devor-Henneman DE, Ward JM, Sundberg JP: Pathology of the gastrointestinal tract of genetically engineered and spontaneous mutant mice. *In:* Pathology of Genetically Engineered Mice, eds. Ward JM, Mahler JF, Maronpot RR, Sundberg JP, pp. 269-298. Iowa State University Press, Ames, IA, 2000
11. Masuno K, Yanai T, Hirata A, Yonemaru K, Sakai H, Satoh M, Masegi T, Nakai Y: Morphological and immunohistochemical features of *Cryptosporidium andersoni* in cattle. Vet Pathol **43:**202-207, 2006
12. Park JH, Seok SH, Baek MW, Lee HY, Kim DJ, Park JH: Gastric lesions and immune responses caused by long-term infection with *Helicobacter heilmannii* in C57BL/6 mice. J Comp Pathol **139:**208-217, 2008
13. Poytner D, Selway SAM, Papworth SA, Riches SR: Changes in the gastric mucosa of the mouse associated with long lasting unsurmountable histamine H_2 blockade. Gut **27:**1338-1346, 1986
14. Rehm S, Sommer R, Derberg F: Spontaneous nonneoplastic gastric lesion in female Han:NMRI mice and influence of food restriction throughout life. Vet Pathol **24:**216-225, 1987
15. Ward, JM, Yoon M, Anver M, Haines DC, Kudo G, Gonzalez FJ, Kimura S: Hyalinosis in Ym1/Ym2 gene expression in the stomach and respiratory tract of 129S4/SvJae and wild-type and CYP1A2-null B2,129 mice. Am J Pathol **158:**323-332, 2001

CASE III: Novartis case #2 (AFIP 3134885).

Signalment: Male, spontaneously hypertensive (SH) rat (*Rattus norvegicus*).

History: The rat was found to be dorsally recumbent, with head tilting to the right and nystagmus of the left eye.

Gross Pathology: Pale, finely pitted kidneys.

Histopathologic Description: Kidney: The renal capsular surface is diffusely undulant, with multiple shallow cortical indentations and multifocal tubular ectasia. Cortical indentations are often associated with perivascular cortical interstitial expansion and basophilia that correlate to an inflammatory cellular infiltrate comprised of small to moderate numbers of lymphocytes and macrophages, and a few light yellow brown pigment-laden macrophages (presumed hemosiderophages). The leukocytic infiltrate is multifocally accompanied by enhanced prominence of blood vessels, occasional hemorrhage, minimal to mild fibrosis, and separation/compression/loss of renal tubules. Renal proximal tubules and collecting ducts are multifocally ectatic with proteinaceous casts. In lesser affected tubules, the epithelium contains modest numbers of hyaline droplets. Other tubules exhibit sloughing of renal tubular epithelium (degeneration), presence of cellular and karyorrhectic debris (necrosis) and cellular and granular casts. Many scattered renal tubules exhibit tubular basophilia (regeneration). A few tubules also have thickened basement membranes. Glomeruli in markedly affected areas are often closely arranged due to tubular drop out. Multifocally, basement membranes of glomerular tufts and capsules are thickened and fibrotic (glomerulosclerosis) (**figs. 3-1 and 3-2**). Multiple arcuate and/or interlobular arteries in the renal cortex exhibit reduction of vascular lumen, intimal deposits and medial smooth muscle hyperplasia with occasional degeneration of medial smooth muscle (**fig. 3-3**). The pelvic lamina propria has multifocal infiltrates of lymphocytes.

Contributor's Morphologic Diagnosis: Nephro–pathy, chronic, marked, with multifocal lymphohistiocytic interstitial nephritis, glomerular and tubular basement membrane thickening, glomerulosclerosis, tubular degeneration/necrosis/regeneration, tubular ectasia, casts and hyaline droplets, and arterial smooth muscle hyperplasia and degeneration.

Contributor's Comment: The case represents chronic progressive nephropathy (CPN) in rats, which is common in old, male, Sprague-Dawley or Fischer 344 rats fed high protein diets.[4] CPN is a combination of both degenerative and proliferative lesions, and basophilic tubules are considered to be an early lesion in this nephropathy.[2,3] In chronic studies, the proliferative components of CPN may need to be discriminated from pre-neoplastic proliferative changes.[2] Degenerative lesions similar to those observed in this case could result from infections, degenerative nephrosis or toxic insults. However, the inciting factor is often difficult to discern by histologic evaluation. The vascular changes observed in this case may be related to the rat being spontaneously hypertensive and may have

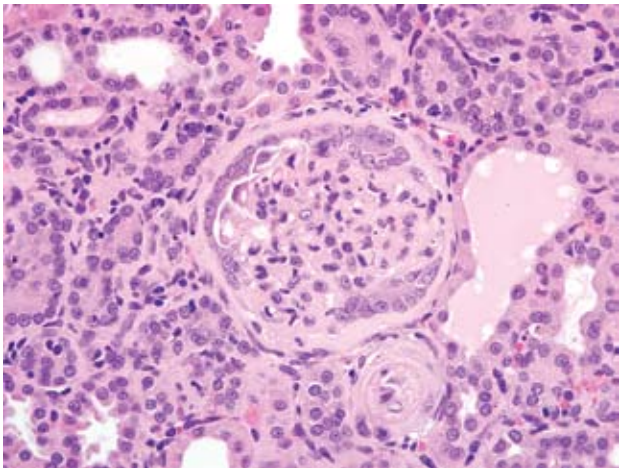

3-1. Kidney, rat. Glomeruli within the cortex often have thickened capillary loops, increased mesangium within the glomerular tuft, and hyperplastic parietal epithelium with multifocal synechiae. (HE 400X)

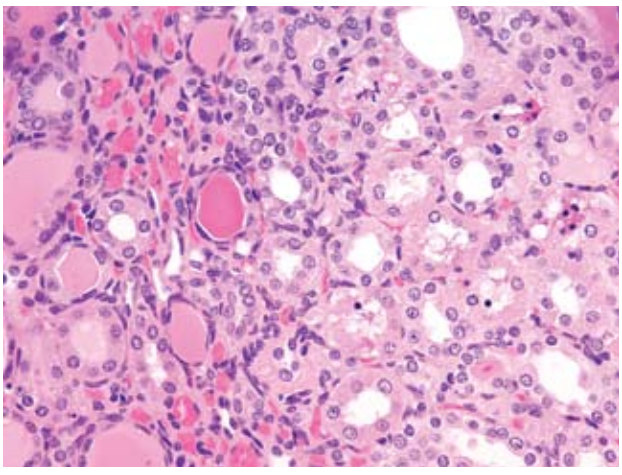

3-2. Kidney, rat. Multifocally, cortical tubular epithelium is attenuated, necrotic, or regenerative, and tubular lumina often contain abundant brightly eosinophilic proteinaceous material. (HE 400X)

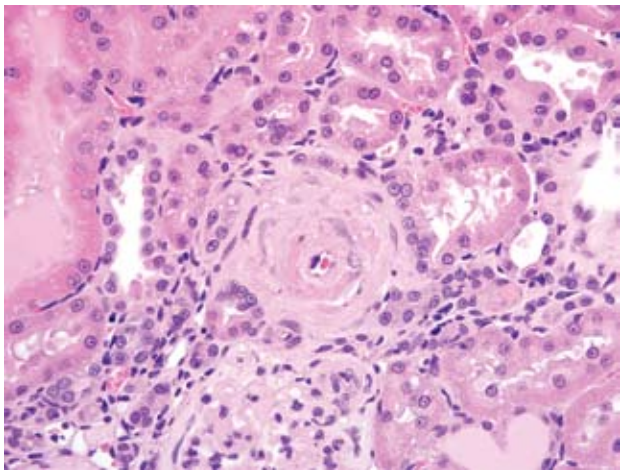

3-3. Kidney, rat. Arterioles within the cortex are often surrounded by concentric layers of fibrosis; the tunica media of these vessels is expanded by eosinophilic material, and the endothelium is hypertrophied. (HE 400X)

contributed to the development of the renal lesions.[1,2] Vascular lesions are typically not described in cases of CPN. Hence, in other strains, polyarteritis nodosa would be a good differential.

AFIP Diagnosis: 1. Kidney: Glomerulonephropathy, diffuse, chronic, marked, characterized by glomerular sclerosis and synechia, tubular atrophy, degeneration, necrosis, regeneration, ectasia, and proteinosis, and interstitial fibrosis and nephritis.

2. Kidney, cortex: Arteriolosclerosis, proliferative, multifocal, moderate, with medial degeneration and necrosis, and smooth muscle hyperplasia.

Conference Comment: In addition to the lesions described above, several conference participants' slides contained fibrinoid necrosis in multiple affected vessels. As mentioned by the contributor, vascular lesions are not typical of CPN, so their presence should raise the index of suspicion for another cause, such as strain phenotype. Recognized risk factors for the development of CPN in rats include the following:[3]

1. Age: greater than 12 months
2. Sex: male
3. Strain: Sprague-Dawley or Fischer 344
4. Diet: high protein and/or total caloric intake
5. Mesangial IgM deposition
6. Elevated prolactin levels

Conference participants discussed the importance of CPN as a potential confounder in laboratory investigations in general, and in two-year carcinogenicity assessments in particular, as alluded to by the contributor. The earliest changes, i.e. basophilic tubules with thickened basement membranes, may be present in kidneys of rats as young as two months of age. In advanced stages, the proliferative lesions of CPN may be difficult to distinguish from preneoplastic hyperplastic lesions, termed atypical tubule hyperplasia (ATH). Specific criteria to make this important distinction have been proposed, and are summarized in the table below:[2]

	Simple Tubule Hyperplasia	**Atypical Tubule Hyperplasia**
Significance	Compensatory regenerative response to cellular injury and loss	Preneoplastic developmental stage in a continuum with renal tubule adenoma/carcinoma
Cytoplasm	Basophilic	Mostly basophilic "glassy" cytoplasm; esoniophilic, clear, chromophobic, and oncocytic forms also described
Histomorphology	Thickened basement membrane; increased number of epithelial cells; extends laterally but not generally inward beyond the single layer of tubule lining	Proliferation beyond a single layer of tubular epithelium to form a solid tubule profile; expands into surrounding matrix and partially surrounded by rim of connective tissue cells; transition to early adenoma when proliferation extends beyond the nephron integrity

Contributor: Novartis Institutes for BioMedical Research, One Health Plaza, East Hanover, New Jersey 07836
http://www.nibr.com/

References:

1. Feld LG, Van Liew JB, Galaske RG, Boylan JW: Selectivity of renal injury and proteinuria in the spontaneously hypertensive rat. Kidney Int **12:**332-343, 1977
2. Hard GC, Seely JC: Recommendations for the interpretation of renal tubule proliferative lesions occurring in rat kidneys with advanced chronic progressive nephropathy (CPN). Toxicol Pathol **33:**641-649, 2005
3. Hill GS: Hypertensive nephrosclerosis. Curr Opin Nephrol Hypertens **17:**266-270, 2008
4. Percy DH, Barthold SW: Pathology of Laboratory Rodents and Rabbits, 3rd ed., pp. 161-162. Blackwell Publishing, Ames, IA, 2007

CASE IV: 09-468 (AFIP 3138312).

Signalment: Approximately 12-week-old, male, acid sphingomyelinase knockout (asmase$^{-/-}$) mouse (*Mus musculus*) on C57BL/6 background.

History: Recent onset of weakness, twitching, and shaking.

Gross Pathology: This mouse presented in thin body condition. The liver was mildly enlarged and mottled pale tan and yellow. No adipose tissue was present in the abdominal cavity.

Laboratory Results:
Hematology:
Manual Differential:

- Manual Neutrophil %: 46 (3-22.5)
- Band %: 3
- Manual Lymphocyte %: 29 (69-93.5)
- Manual Monocyte %: 4 (0-8)
- Others %: 18
- WBC Morphology (reported by technician): Atypical cells that are classified as others are variable in size ranging from 5 to 20 um. The nucleus of these cells is irregular in shape. Some are angular, others indented, and some are folded. The nuclear chromatin material is clumped in some of the cells and smooth in others.
- Cytoplasm varies from being scant to moderate. In some of the cells the cytoplasm resembles that of a monocyte.
- RBC Morphology: RBC morphology is within normal limits.
- Platelet Morphology: No abnormality noted.

CBC with automatic differential:

- Red Blood Cells: 9.04 (8.2-10.4)
- Hemoglobin: 14.6 (14.5-16.2)
- Hematocrit: 41.7% (38.5-46.0)
- MCV: 46.1 fL (42-48)
- MCH: 16.1 pg (14.5-16.2)
- MCHC: 35.0 g/dL (31.4-36.8)
- RDW: 19.8% (13.8-17.0)
- Platelets: 445 K/uL (799-1,300)

Chemistry (liver panel):

- ALP: 83 IU/L (23-181)
- ALT (SGPT): 110 IU/L (16-58)
- AST (SGOT): 1551 IU/L (36-102)
- GGT: 0.0 IU/L (0-2)
- Total Bilirubin: 0.3 mg/dl (0.0-0.3)
- Total Protein: 5.1 g/dl (4.1-6.4)
- Albumin: 3.2 g/dl (2.5-3.9)
- Blood Urea Nitrogen: 27 mg/dl (14-32)
- Creatinine: 0.3 mg/dl (0.1-0.6)
- B/C Ratio: 90.0 (21-127)

Histopathologic Description: **Brain**: There is a moderate to marked loss of Purkinje cells that is most severe in the anterior lobes of the cerebellum. Some remaining Purkinje cells are undergoing degeneration and necrosis, with shrinkage, hypereosinophilia, and nuclear pyknosis (**fig. 4-1**). Most of the remaining Purkinje cells and many other neurons throughout the brain contain well-delineated, small, lipid-containing vacuoles. There is mild to moderate multifocal gliosis, with an infiltrate of lipid-laden gitter cells. Many choroid plexus cells also contain lipid-laden vacuoles within their cytoplasm (**fig. 4-2**).

Lung: There is a moderate to marked diffuse intraalveolar infiltrate of macrophages, the cytoplasm of which is moderately to markedly distended with foamy vacuolation (lipid). Many macrophages also contain eosinophilic crystalline material within their cytoplasm, and similar material is present extracellularly within alveolar spaces (**fig. 4-3**). Occasional multinucleated giant cells and neutrophils are present, particularly in more severely affected areas. In more severely affected areas, there is an intraalveolar infiltrate of fibrin, and in the most severely affected areas, alveoli are filled with macrophages,

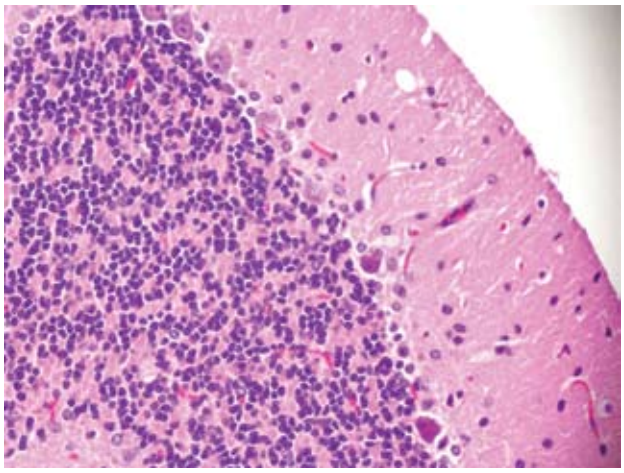

4-1. Cerebellum, mouse. There is a moderate to marked loss of Purkinje cells that is most severe in the anterior lobes of the cerebellum. Some remaining Purkinje cells are undergoing degeneration and necrosis, with shrinkage, hypereosinophilia, and nuclear pyknosis. Most of the remaining Purkinje cells and many other neurons throughout the brain contain well-delineated, small, lipid-containing vacuoles. Photomicrograph courtesy of Memorial Sloan Kettering Cancer Center, 1275 York Ave., Box 270, New York, NY 10021, monettes@mskcc.org.

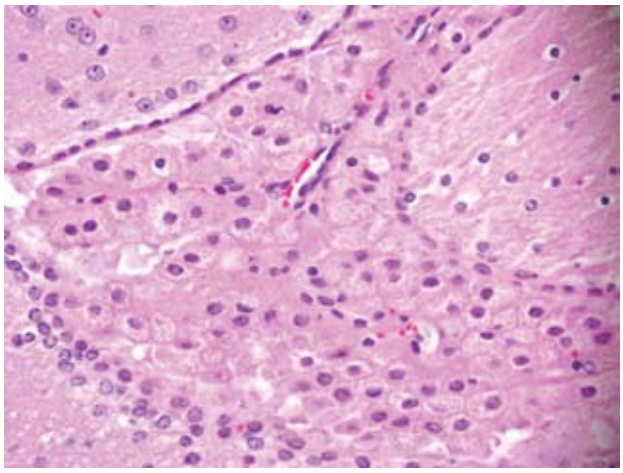

4-2. Brain, mouse. Many choroid plexus cells contain lipid-laden vacuoles within their cytoplasm. Photomicrograph courtesy of Memorial Sloan Kettering Cancer Center, 1275 York Ave., Box 270, New York, NY 10021, monettes@mskcc.org.

crystalline material, and fibrin, with loss of air spaces. Interstitial connective tissue is moderately expanded by edema.

Infiltrates of vacuolated macrophages were also present within the bone marrow, liver, adrenal gland, thymus, thyroid, epididymis, preputial gland, mesenteric lymph node, and myocardium. Vacuolation was also present within ganglion cells adjacent to the heart and neurons within the spinal cord, as well as follicular epithelial cells of the thyroid, epithelial cells of the epididymis, and renal tubular epithelial cells.

Contributor's Morphologic Diagnosis: 1. Lung: Alveolar histiocytosis, diffuse, moderate to marked, with intracytoplasmic lipid.
2. Lung: Eosinophilic crystalline pneumonia, regionally extensive, moderate, with intraalveolar fibrin.
3. Brain, cerebellum: Purkinje cell necrosis and loss, diffuse, moderate to marked.
4. Brain: Neuronal vacuolation, diffuse, moderate.
5. Brain: Gliosis, multifocal, mild to moderate, with gitter cells containing intracytoplasmic lipid.

Contributor's Comment: Sphingomyelin is the main lipid constituent of the plasma membrane and plasma-membrane-derived membranes (e.g. endosomes, lysosomes).[7] Lysosomal acid hydrolases (such as acid sphingomyelinase) play an important role in the turnover of membrane lipids from any cell. Acid sphingomyelinase (ASM) is present in endosomes and lysosomes of all cells, particularly the reticuloendothelial cells of the liver, spleen, bone marrow, lung, and macrophages. During times of cell stress, ASM is translocated from lysosomes to the outer leaflet of the cell membrane, where it functions to hydrolyze sphingomyelin into ceramide and phosphocholine.[2] Ceramide stimulates reorganization of membrane rafts (composed of sphingolipids and cholesterol) into larger, ceramide enriched 'platforms', thus bringing together signaling proteins and causing downstream changes within the cell.[2,11] Documented roles and potential roles of ceramide include phosphorylation/dephosphorylation of intracellular signaling molecules, calcium transport across membranes, cell differentiation, mitogenesis, inflammatory mediation (primarily through TNF-induced signaling), immune responses, and apoptosis.[4] Types of cell stress documented to cause ASM translocation to the cell membrane (with resulting ceramide formation) include irradiation, conjugation of cell surface receptors, heat shock, and exposure of cells to bacterial pathogens, to name a few.[11] The roles of ASM and ceramide in cell responses to these stressors is supported by the fact that ASM knockout (ASMKO) mice are resistant to cell death induced by irradiation and ischemia, and are resistant

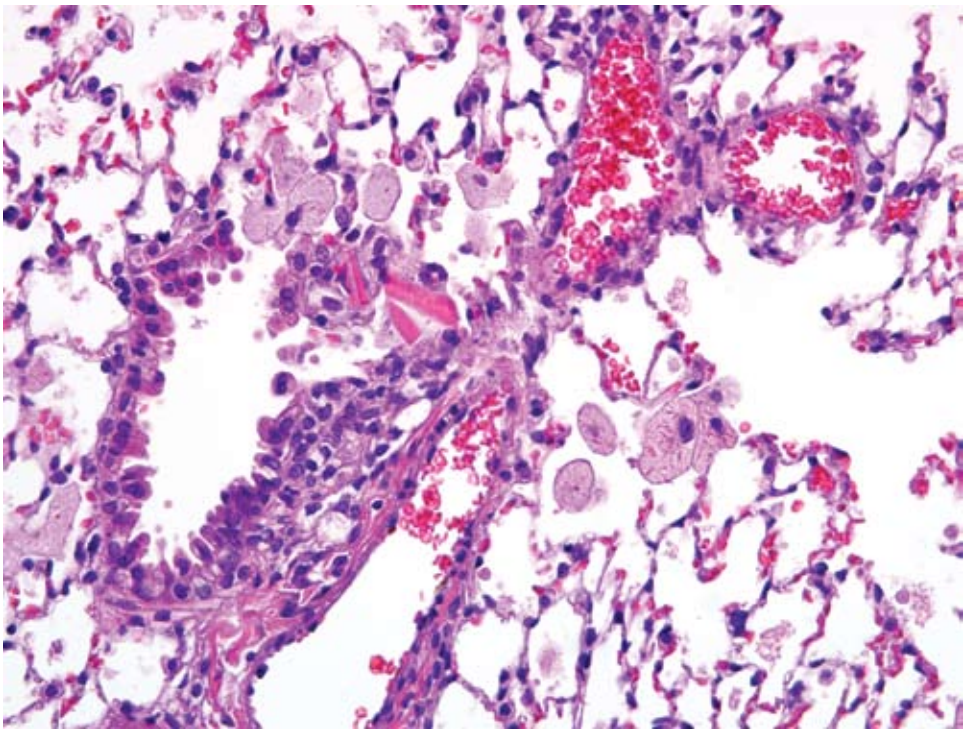

4-3. Lung, mouse. Within alveolar lumina there are numerous large, lipid-laden alveolar macrophages. Multifocally within terminal bronchioles and alveoli there are brightly eosinophilic rectangular crystals; similar eosinophilic crystalline material is occasionally found within the cytoplasm of macrophages. (HE 400X)

to infection by various pathogens (often because the organisms are unable to cross the cell membrane).

In humans, an inherited (autosomal recessive) deficiency of ASM activity results in A and B forms of Niemann-Pick disease (NPD).[4,7] Over a dozen mutations cause defects in the ASM enzyme leading to NPD types A and B. Type A NPD is a severe neurodegenerative disorder leading to death by 3 years of age. Individuals with this form of the disease have very little (<5%) ASM activity. In type B NPD, there is little to no neurological involvement, and individuals often survive into adulthood. The decreased severity of clinical signs in these patients is thought to be due to variable amounts (>5%) of ASM activity.[7] A third form of NPD, type C, is also a lipid storage disease, but is due to mutation in unrelated genes (called NPC-1 or NPC-2).

In ASMKO mice, the disease is also autosomal recessive, and the phenotype of affected mice is essentially identical to humans with type A NPD.[4] Mice are normal at birth, with ataxia and tremors beginning at approximately 8 weeks of age. There is rapid disease progression, with lethargy, decreased responses to stimuli, and difficulty eating by 12-16 weeks of age. Severe ataxia is also generally present by 16 weeks of age. Death usually occurs by 6-8 months of age. Biochemical analysis of homozygous ASMKO mice reveals no detectable ASM activity in any tissues tested (i.e. liver, lung, spleen, kidney, heart, brain). Lipid analysis of liver and brain showed approximately 15 and 5-fold increases, respectively in sphingomyelin. Total blood cholesterol levels are elevated approximately 80% in these mice, and nearly all of this is associated with the high density lipoprotein (HDL) fraction. Heterozygotes have approximately 50% ASM activity and present with no clinical disease.

Reported gross pathology findings in ASMKO mice at the time of naturally-occurring death included a hunched appearance, 50% loss in body and brain weight, and hepatosplenomegaly. Histopathologically, lipid-laden foam cells (so-called NPD cells) were present in most major organs. Electron microscopic evaluation revealed multilamellar cytoplasmic inclusions in all tissues, especially the brain. Additionally, Purkinje cell loss and atrophy of the cerebellum and midbrain were present. The neuronal activity of Purkinje cells far exceeds most other cell types in the CNS, and they form excitatory and inhibitory synapses and relay sensory information from all parts of the body.[7] This high activity level leads to rapid membrane turnover, and this has been hypothesized to account for their increased rate of death in comparison with other neurons in the CNS. This hypothesis is supported by the observation that Purkinje cell loss occurs in the anterior lobules of the cerebellum first, with preservation of the posterior lobular neurons until late in the course

of the disease. Posterior lobular Purkinje cells contain high levels of sphingosine kinase, which may serve as an alternate mechanism for sphingolipid breakdown.

In addition to neuronal disease, both humans with types A and B NPD and ASMKO mice are reported to develop lung pathology. In human type A NPD, neurodegeneration usually causes death before pulmonary disease becomes advanced. However, individuals with the type B form may show progressive pulmonary dysfunction and respiratory infections that can be fatal.[5] Pulmonary disease is primarily related to alterations of surfactant, which contains increased saturated phosphatidylcholine and sphingomyelin compared to normal individuals. This leads to decreased catabolism by alveolar macrophages (a process that requires lysosomal activity), and subsequent decreased clearance from the lungs. In addition to elevated levels of surfactant, the increased sphingomyelin contributes to abnormal surfactant function. Pulmonary macrophage dysfunction is also thought to play a role in lung disease.[1] Decreased superoxide production by pulmonary macrophages has been documented in ASMKO mice and the addition of ASM *in vitro* increased superoxide production, further supporting the role of ASM in macrophage function. Additionally, ASMKO mice had elevated levels of macrophage inflammatory proteins (MIP), specifically MIP1α (a monocyte chemoattractant) and MIP2 (a neutrophil chemoattractant). These chemokines are normally produced by macrophages and bronchial epithelial cells, leading to increased inflammatory cell recruitment. Histopathologically, alveolar macrophages were most affected by the accumulation of intracellular lipids, but ciliated cells of airways, type I pneumocytes, and endothelial cells were also affected. Interestingly, there was no evidence of fibrosis within affected lungs of ASMKO mice, indicating preservation of normal architecture and potential for normal function if ASM activity is restored.

Eosinophilic crystalline pneumonia commonly occurs in strains on a C57BL/6 background.[3] It may occur spontaneously or in concert with other pulmonary lesions, such as pulmonary adenomas, lymphoproliferative disease, allergic pulmonary disease, and parasitic or fungal infection. The crystals in eosinophilic crystalline pneumonia are composed predominately of Ym1 protein, a chitinase-like protein associated with neutrophil granule products and secreted by activated macrophages. The function of Ym1 protein is not fully understood but is believed to be involved in host immune defense, eosinophil recruitment, and cell-cell and cell-matrix interactions consistent with tissue repair. The mechanism of induction of eosinophilic crystalline pneumonia is unknown.

AFIP Diagnosis: 1. Lung: Alveolar histiocytosis, multifocal, moderate, with intrabronchiolar and intrahistiocytic eosinophilic crystalline material and histiocytic lipid-type cytoplasmic vacuolation.
2. Brain, cerebellum: Purkinje cell degeneration, necrosis, and loss, diffuse, moderate, with gliosis, and neuronal and glial lipid-type cytoplasmic vacuolation.
3. Brain, cerebrum: Neuronal degeneration, necrosis, and loss, diffuse, marked, with gliosis, and neuronal and glial lipid-type cytoplasmic vacuolation.

Conference Comment: The contributor provides an excellent example of the ASMKO phenotype, a concise review of sphingomyelin in plasma membrane physiology, and a complete summary of this knockout and its relevance as a model for NPD in humans. Type A NPD has also been reported in cats and a miniature poodle dog [6], and findings in a Hereford calf with sphingomyelinase deficiency were most consistent with type A NPD.[10] In general, lysosomal storage diseases are characterized by the intracellular accumulation of substrates that cannot be degraded by lysosomes, ultimately resulting in cell death. Several mechanisms explain dysfunction of lysosome-mediated degradation of substrate: 1) mutation resulting in reduced synthesis of lysosomal enzymes; 2) synthesis of dysfunctional or inactive proteins that resemble lysosomal enzymes; 3) misdirection of enzymes to sites other than lysosomes due to defective posttranslational processing; 4) lack of enzyme activators or protector proteins; 5) lack of substrate activator proteins; and 6) lack of transport protein to eliminate digested material from lysosomes.[12] While most cell types are susceptible to the accumulation of substrates, neurons and cardiomyocytes are particularly affected due to their long post-mitotic lifespan. Lysosomal storage diseases are classified as inherited or acquired, and subdivided by the class of macromolecule whose degradation is defective. Clinically, a common theme among the inherited storage diseases is juvenile-onset progressive neurologic dysfunction. The following table summarizes a small selection of the growing list of inherited lysosomal storage diseases described in animals:[8,12]

Macromolecule Class	Lysosomal Storage Disease
Sphingolipidoses	GM_1 gangliosidosis (generalized gangliosidosis) GM_2 gangliosidosis Glucocerebrosidosis (Gaucher disease) Sphingomyelinosis (NPD Types A, B, and C) Galactosialidosis Galactocerebrosidosis (globoid cell leukodistrophy, Krabbe disease)
Glycoproteinoses	α-Mannosidosis β-Mannosidosis α -L-fucosidosis
Mucopolysaccharidoses	Mucopolysaccharidosis types I, III, VI, VII, and others
Glycogenoses	Glycogenosis type II (Pompe disease) Glycogenosis type III (Cori disease) Glycogenosis type IV (Polyglucosan body disease)
Mucolipidoses	Inclusion-cell disease (mucolipidosis II)
Ceroid lipofuscinoses	Neuronal ceroid-lipofuscinosis (Batten disease) (see WSC 2008-2009, Conference 24, Case III)
Miscellaneous	Lafora disease Motor neuron disease of English Pointers

In addition to the C57BL/6 strain, other laboratory mice commonly affected by eosinophilic crystalline pneumonia include 129SvJae and its derivatives, severe combined immunodeficiency (SCID) mice, and knockout mice targeting specific components of the immune system.[3] An example of eosinophilic crystalline pneumonia is available in WSC 2007-2008, Conference 8, Case I.

Focally affecting some sections of lung in this case, alveoli contain small amounts of necrotic cellular debris admixed with low numbers of viable and degenerate neutrophils and macrophages, and the adjacent pleura and alveolar septa are infiltrated by lymphocytes, macrophages, and neutrophils.

Contributor: Memorial Sloan Kettering Cancer Center, New York, NY 10021 http://www.mskcc.org

References:

1. Dhami R, He X, Gordon RE, Schuchman EH: Analysis of the lung pathology and alveolar macrophage function in the acid sphingomyelinase-deficient mouse model of Niemann-Pick disease. Lab Invest **81:**987-999, 2001
2. Gulbins E, Dreschers S, Wilker B, Grassme H: Ceramide, membrane rafts, and infections. J Mol Med **82:**357-363, 2004
3. Hoenerhoff MJ, Starost MF, Ward JM: Eosinophilic crystalline pneumonia as a major cause of death in 129S4/SvJae mice. Vet Pathol **43:**682-688, 2006
4. Horinouchi K, Erlich S, Perl DP, Ferlinz K, Bisgaier CL, Sandhoff K, Desnick RJ, Stewart CL, Schuchman EH: Acid sphingomyelinase deficient mice: a model of types A and B Niemann-Pick disease. Nature Genetics **10:**288-293, 1995
5. Ikegami M, Rajwinder D, Schuchman E: Alveolar lipoproteinosis in an acid sphingomyelinase-deficient mouse model of Niemann-Pick disease. Am J Physiol Lung Cell Mol Physiol **284:**L518-L525, 2003
6. Jolly, RD, Walkley SU: Lysosomal storage diseases of animals: an essay in comparative pathology. Vet Pathol **34:**527-548, 1997
7. Macauley SL, Sidman RL, Schuchman EH, Taksir T, Stewart GR: Neuropathology of the acid sphingomyelinase knockout mouse model of Niemann-Pick: A disease including structure-function studies associated with cerebellar Purkinje cell degeneration. Experimental Neurology **214:**181-192, 2008
8. Maxie MG, Youssef S: Nervous system. *In*: Jubb, Kennedy, and Palmer's Pathology of Domestic Animals, ed. Maxie MG, 5th ed., vol. 1, pp. 322-330. Elsevier

Saunders, Philadelphia, PA, 2007
9. Otterbach B, Stoffel W: Acid sphingomyelinase-deficient mice mimic the neurovisceral form of human lysosomal storage disease (Niemann-Pick disease). Cell **81:**1053-1061, 1995
10. Saunders GK, Wegner DA: Sphingomyelinase deficiency (Niemann-Pick disease) in a Hereford calf. Vet Pathol **45:**201-202, 2008
11. Schuchman EH: The pathogenesis and treatment of acid sphingomyelinase-deficient Niemann-Pick disease. J Inherit Metab Dis **30:**654-663, 2007
12. Zachary JF: Nervous system. *In:* Pathologic Basis of Veterinary Disease, eds. McGavin MD, Zachary JF, 4th ed., pp. 928-930. Mosby Elsevier, St. Louis, MO, 2007